Published in final edited form as:
Hepatology. 2015 January ; 61(1): 129–140. doi:10.1002/hep.27383.

Osteopontin deficiency does not prevent but promotes alcoholic neutrophilic hepatitis in mice

Raul Lazaro[1,2,*], **Raymond Wu**[1,2,*], **Sunyoung Lee**[1,2,*], **Nian-Ling Zhu**[1,2], **Chia-Lin Chen**[1,3], **Samuel W. French**[1,4], **Jun Xu**[1,2], **Keigo Machida**[1,3], and **Hidekazu Tsukamoto**[1,2,5]

[1]Southern California Research Center for ALPD and Cirrhosis

[2]Department of Pathology, Keck School of Medicine of the University of Southern California

[3]Department of Molecular Microbiology and Immunology, Keck School of Medicine of the University of Southern California

[4]Harbor-UCLA Medical Center, Los Angeles, California, USA

[5]Department of Veterans Affairs Greater Los Angeles Healthcare System, Los Angeles, California, USA

Abstract

Alcoholic hepatitis (AH) is a distinct spectrum of alcoholic liver disease (ALD) with intense neutrophilic (PMN) inflammation and high mortality. Although a recent study implicates osteopontin (SPP1) in AH, SPP1 is also shown to have protective effects on experimental ALD. To address this unsettled question, we examined the effects of SPP1 deficiency in male mice given 40% calories derived from *ad libitum* consumption of the Western diet high in cholesterol and saturated fat (HCFD) and the rest from intragastric feeding (*iG*) of alcohol diet without or with weekly alcohol binge. Weekly binge in this new hybrid feeding model shifts chronic ASH with macrophage inflammation and perisinusoidal and pericelluar fibrosis to AH in 57% (15/26) of the mice, accompanied by inductions of chemokines (*Spp1*, *Cxcl1*, *Il-17a*), progenitor genes (*Cd133*, *Cd24*, *Nanog*, *Epcam*), PMN infiltration, and clinical features of AH such as hypoalbuminemia, bilirubinemia, and splenomegaly. SPP1 deficiency does not reduce the AH incidence and inductions of progenitor and fibrogenic genes but rather enhances the *Il-17a* induction and PMN infiltration in some mice. Further, in the absence of SPP1, chronic ASH mice without weekly binge begin to develop AH. In conclusion, these results suggest SPP1 has a protective rather than causal role for experimental AH reproduced in our model.

Keywords

TLR4; NANOG; Spp1; IL-17a; IL-22

Since the first description by Gordon Beckett and colleagues in 1961, alcoholic hepatitis (AH) has been recognized as a distinct and clinically most challenging spectrum of alcoholic

Address correspondence to: Hidekazu Tsukamoto, University of Southern California, 1333 San Pablo Street, MMR-402, Los Angeles, CA 90033. TEL: 323-442-5107; FAX: 323-442-3126; htsukamo@med.usc.edu.
*Equally contributed.

liver disease (ALD) with a 28-day mortality of 30–50% accounting for up to 20% of patients with heavy alcohol intake (1–4). Although AH is presented with acute inflammation, chronic alcoholic steatohepatitis (ASH) with liver fibrosis often co-exists (3). AH resulted in 56,809 hospital admissions in the US in 2007 (4) and continues to be a major cause of mortality and morbidity worldwide (5). For this reason, there is an urgent need for better understanding of the AH pathogenesis and development of improved management and therapies for the disease (1, 5–7).

Undoubtedly, the lack of an animal model which reproduces key features of AH, has been a major obstacle for advancement of our knowledge concerning the AH pathogenesis. Histologically, AH is characterized by intense PMN infiltration into the parenchyma often around foamy hepatocytes, Mallory hyaline inclusions, and the background of chronic fibrotic changes ranging from pericellular, perisinusoidal, bridging fibrosis to cirrhosis (7). Clinically, the AH patients exhibit bilirubinemia, hypoalbuminemia, coagulopathy, portal hypertension, and in severe cases, sepsis, renal failure, hepatic encephalopathy (1–4). Life-style factors and co-morbidities are important considerations. Obesity and Western diet synergistically promote ALD including AH (8–10), and diabetes which is a common consequence of obesity is a comorbidity in 20–30% of AH patients (10). Concomitant HCV or HBV infection is a well-known promoter of ALD (11, 12) including AH (13). Heavy drinkers who dramatically increase alcohol intake or binge drink are also at high risk (1, 14, 15).

Thus, in designing a development of an AH animal model, one must incorporate these risk factors to assess whether both histological and clinical features are reproduced. Intragastric (*iG*) ethanol feeding which achieves alcohol intake of heavy drinkers (16), induces synergistic ASH with M1 macrophage activation in overfed obese mice (10) and zonal necrosis and inflammation in HCV *NS5A* transgenic mice (17). Binge alcohol intake after 10 days of feeding an ethanol liquid diet, causes a transient increase in plasma ALT and liver PMN followed by normalization of these changes within 2–3 days and there is no evidence of chronic pathology (18, 19). In essence, these models fail to reproduce intense PMN parenchymal infiltration in the background of chronic liver pathology typically seen in AH. In approaching this challenge in the present study, we first incorporated two of the AH risk factors by “hybrid” feeding via *iG* feeding assuring sustained alcohol intoxication and *ad libitum* feeding of Western diet. This model resulted in severe chronic ASH with mononuclear cell (MNC) inflammation, pericellular and perisinusoidal fibrosis. When we added weekly alcohol binge to this model without altering other variables including total alcohol intake, it reproduced key histological and clinical changes of AH.

Osteopontin (SPP1) is a multi-functional protein secreted by various cell types including macrophages, PMN, fibroblasts, biliary epithelial cells, and hepatocytes and is induced in experimental models of ASH and in ALD patients (20–23). Because it is a potent chemoattractant for PMN (24) and promotes liver fibrosis in non-alcoholic steatohepatitis (25), the pathogenetic roles of SPP1 in ASH and AH are proposed. Hepatic PMN infiltration in alcohol-fed female rats subjected to single LPS injection, is ameliorated by administration of SPP1 neutralizing antibody (22) and *Spp1*−/− mice are protected from experimental alcoholic liver injury with reduced steatosis, inflammatory cytokine expression, PMN

infiltration, and plasma ALT (21). In contrary, protective roles of SPP1 are also reported. Transgenic expression of SPP1 in hepatocytes, reduces alcohol-induced hepatic steatosis, balloon cell degeneration, lipid peroxidation, inflammation, and plasma ALT (26). Treatment with milk SPP1 preserves intestinal integrity, prevents leaky gut and LPS translocation, and attenuates early alcoholic liver injury including PMN infiltration (27). To address this unresolved question on the role of SPP1 in chronic ASH and AH, we have tested *Spp1*−/− mice in our newly developed hybrid models. Our results demonstrate SPP1 deficiency fails to prevent AH incidence in the AH model and tends to increase the number of PMN infiltrating into the liver. More strikingly, the chronic ASH model which does not develop AH in wild type (WT) mice begins to exhibit PMN infiltration in *Spp1*−/− mice even without binge, suggesting the protective role of SPP1.

Materials and Methods

(additional methods described in Suppl. Information)

Animal models

The animal protocol for this study was approved by the Institutional Animal Care and Use Committee at the University of Southern California. Male C57B/6 mice were fed solid Western diet high in cholesterol and saturated fat (HCFD) (Dyets Inc., #180724) or regular chow *ad libitum* for 2 wk followed by implantation of the *iG* catheter and *iG* feeding of ethanol and a high fat liquid diet (corn oil as 36% Cal) as described (16) at 60% of total daily caloric intake. Mice consumed the remaining 40% Cal via *ad libitum* intake of HCFD or chow. The ethanol dose was increased to 27 g/kg/day over a 8 wk-period and pair-fed control mice were fed isocaloric high fat liquid diet. Thus, this hybrid model of *ad libitum* and *iG* feeding, generated the following 4 groups: Chow+Cont, Chow+Alc, HCFD+Cont, HCFD+Alc. Additionally, Chow+Alc and HCFD+Alc mice were subjected to alcohol binge at a weekly interval from the 2nd week of *iG* feeding (Fig. 1). For this binge, ethanol *iG* infusion was withdrawn for 5~6 hr and a bolus dose (4~5g/kg) of ethanol equivalent to that was withdrawn, was given (Chow+Alc+Binge and HCFD+Alc+Binge). To test the role of SPP1 in chronic ASH and AH, *Spp1*−/− (Jackson Lab) and congenic wild type (WT) mice were subjected to the identical HCFD+Alc or HCFD+Alc+Binge regimen. At 1pm of the last day of the experiments, the animals were anesthetized, venous blood collected, entire liver and spleen removed, weighed, and livers processed for analyses.

Results

HCFD and alcohol synergistically induce Chronic ASH

With *iG* feeding of a liquid high fat diet plus ethanol or isocaloric dextrose at 60% of daily caloric intake, the mice continued to consume *al libitum* chow or HCFD, and their caloric intake from chow and HCFD were not different among the different groups (Suppl. Table 1). Body weights (BW) and BALs determined in the end of the 8-wk hybrid feeding, are also summarized in Suppl. Table 1. Only the HCFD+Cont group had significantly increased end BW compared to other groups. With the low final dose of ethanol at 27 g/kg/day, average BALs increased only to 89mg/dL in Chow+Alc and 117mg/dL in Chow+Alc

+Binge, but elevated to 434mg/dL in HCFD+Alc and 263 mg/dL in HCFD+Alc+Binge, depicting the marked enhancing HCFD effect on BALs which is attenuated by binge (discussions in Suppl. Information). Chow+Cont and HCFD+Cont mice had normal liver weight/BW ratio (LW/BW) and plasma AST and ALT (Fig. 2A). Liver histology of Chow +Cont was normal and HCFD+Cont showed small fat droplets in zone 1 and 2 hepatocytes (Fig. 2B) with a mild increase in liver triglyceride level (Suppl. Table 1). Chow+Alc mice had modest increases in LW/BW and plasma ALT (Fig. 2A) and mild fatty liver (Fig. 2B, Suppl. Table 1). Chow+Alc+Binge also had a mild hepatomegaly (Fig. 2A) and increased steatosis but without any inflammation (Fig. 2B). In contrast, HCFD+Alc mice showed a 3-fold increase in LW/BW, marked elevations of plasma AST and ALT (Fig. 2A) and liver triglycerides (Suppl. Table 1), and severe ASH accompanied by MNC inflammation, occasional PMN infiltration, and perisinusoidal and pericellular liver fibrosis primarily in zone 2 and 3 (Fig. 2B), demonstrating synergistic effects of the hybrid HCFD and alcohol feeding on the genesis of chronic ASH.

Repeated binge shifts chronic ASH to AH

Before testing weekly binge on the hybrid model, a pilot study was performed to assess the effects of a single binge vs. two-repeated weekly binges after 4–5 wk of the hybrid HCFD +Alc feeding. This study revealed only PMN congestion after the single binge and minimal parenchymal PMN infiltration after the two binges (data not shown). Based on these results, we rationalized that repeated binge may be required for PMN infiltration into the liver parenchyma. Indeed, seven weekly binge episodes in HCFD+Alc+Binge mice, resulted in pathophysiologic changes we did not observe in other groups including splenomegaly, hypoalbuminemia, and bilirubinemia (Fig. 2A). The increase in plasma ALT levels was attenuated compared to HCFD+Alc, but AST levels were equally elevated, resulting in a 2-fold increase in the AST/ALT ratio (0.79+0.16 vs. 0.39+0.09, $p<0.05$). The liver of the HCFD+Alc+Binge mice often looked grossly enlarged and inflamed (Fig. 2C-i and Suppl. Fig 1A), and more importantly, parenchymal PMN infiltration was histologically detected in 57% and intense and diffuse PMN infiltration in zone 2 and 3 of 34% of the mice (in 15 and 9 of 26 mice generated from three separate experiments, respectively). The PMN infiltration as validated by chloracetate esterase (CEA) stain (Fig. 2C-ii and iii), was presented as aggregates of PMN surrounding degenerative fat-loaded hepatocytes or fat globules released by dead hepatocytes (Fig. 2C-iv–vii). In the livers with AH lesions, Sirius red staining was increased (Fig. 2C-viii and ix, Suppl. Fig. 1B). Fibrogenic genes such as 1(I) procollagen (*Col1a1*), -smooth muscle actin (*Acta*), and tissue inhibitor for metalloproteinase 1 (*Timp1*) were also upregulated to much greater degrees in the livers of HCFD+Alc+Binge than HCFD+Alc mice (Fig. 2D). qPCR analysis of the liver RNA also shows conspicuous upregulation of myeloperoxidase (*Mpo*) along with Gro-α (*Cxcl1*) and osteopontin (*Spp1*), the two key chemokines implicated in PMN inflammation in AH (20, 21,28, 29) (Fig. 3A). *Cd68* was increased 7-fold in the HCFD+Alc, validating macrophage inflammation in this chronic ASH model, but markedly reduced in the HCFD+Alc+Binge mice. Inductions of SPP1 and MPO in HCFD+Alc+Binge were also confirmed at the protein levels (Fig. 3B). These results corroborate the histological evidence of PMN infiltration and suggest the possible roles of *Cxcl1* and *Spp1*. We also performed IF microscopy for SPP1 (OPN) and confirmed mild and marked inductions of SPP1 in HCFD+Alc and HCFD+Alc+Binge liver

sections, respectively (Fig. 3C). The specificity of the staining is supported by the absence of the staining in the liver of *Spp1*−/− mouse subjected to HCFD+ALC+Binge. Higher magnification of dual staining for SPP1 and albumin reveals hepatocytes positively stained for both, frequently around intracellular fat vesicles in the HCFD+Alc+Binge WT mouse (arrows in left bottom image of Fig. 3C). SPP1 staining was also present in cells positive for desmin (DES, arrowhead in right bottom image, Fig. 3C), suggesting hepatic stellate cells also express SPP1 in the AH model.

IL-17 and IL-22 are produced by Th17 cells to balance pro-inflammatory vs. hepatoprotective effects (30). IL17 is implicated in chronic inflammatory diseases including ALD (31) and liver fibrosis (32) while IL-22 renders anti-apoptotic effects toward epithelial cells including hepatocytes (33, 34), promotes liver progenitor cell proliferation (35), and inhibits liver fibrosis (36). Our qPCR analysis for these two cytokines revealed a 6.5-fold upregulation of *Il-17a* and a severe depletion of *Il-22* in the livers of the HCFD+Alc+Binge mice (Fig. 3D), suggesting the reciprocally regulated expression of these cytokines in the pathogenesis of AH. In fact, the number of PMN infiltrated into the parenchyma correlated with the extent of *Il-17a* mRNA induction, and the mice which did not develop AH had no or minimal *Il-17a* upregulation (Suppl. Fig. 2A). Hepatic *Il-22* was also reduced in Chow +Alc and Chow+Alc+binge mice but no significant changes in *Il-17a* were noted in these groups (Fig. 3D).

Global induction of PMN, progenitor cell, and cancer-related genes in AH

To globally characterize gene expression profiles associated with the remarkable shift of liver pathology from chronic ASH to AH, liver RNA samples from HCFD+Alc and HCFD +Alc+Binge were subjected to a microarray analysis (Suppl. Table 2). Ingenuity pathway analysis of the data showed clusters of genes involved in progenitor cells and cancer, inflammation, and connective tissue diseases were upregulated while those for drug metabolism, lipid metabolism, and transport are downregulated. (Table 1A). In fact, eight of top 10 most upregulated genes in the AH vs. ASH livers were PMN-related (Table 1B), further supporting the intense PMN response in the AH model. Progenitor cell and cancer-related genes such as *Epcam*, *Cd24*, *Anilin*, *Sox4* were induced in the AH mouse livers (Suppl. Table 2), recapitulating the changes reported to serve as poor prognostic indicators in AH patients (37). Conversely, a group of drug metabolism genes including *Cyp4a12a*, *Cyp4a12b*, *Cyp2c38*, *Ugt2a3*, was suppressed in the HCFD+Alc+Binge livers (Suppl. Table 3), suggesting impaired hepatic lipid and xenobiotic metabolism.

TLR4 induction and activation TLR4/AFP positive cells in experimental AH

As a potential mechanism of the PMN chemokine induction and PMN inflammation in the HCFD+Alc+Binge mice, TLR4 expression and activation were examined by TLR4 IB and co-IP for TRAF6-TAK1 interaction (Fig. 4A). Assessment of these parameters by densitometric quantification, normalization to the loading control, and comparison to the Chow+Control, revealed that TLR4 expression and activation are increased most in the HCFD+Alc+Binge mouse livers (Fig. 4A, lower graphs). As expected, plasma endotoxin concentrations were elevated in HCFD+Alc+Binge mice on the next day after the final

binge (1.7+0.6 U/ml, $p<0.05$) as compared to HCFD+Alc (0.5+0.3U/ml) or other groups (<0.2U/ml).

Ectopic TLR4 activation is also implicated in alcohol-associated liver tumor development and the genesis of NANOG-dependent CD133+ tumor-initiating stem cell-like cells (TICs) (17, 38). The qPCR analysis indeed confirms selective induction of *Cd133* and *Nanog* in the HCFD+Alc+Binge livers (Fig. 4B). To assess the cellular localization of TLR4 and NANOG expression, we performed IF microscopy. In Chow+Cont livers, TLR4 is primarily expressed in sinusoidal cells presumably Kupffer cells with no NANOG expression (Fig. 4C-i). There is a modest increase in TLR4 staining in HCFD+Alc with the sinusoidal pattern (Fig. 4C-iv). In HCFD+Alc+Binge, TLR4 induction is intensified in the inflamed parenchyma along with NANOG-positivity (Fig. 4C-vii), and a high-power view reveals scattered small cells positive with NANOG and TLR4 around hepatocytes with large intracellular fat vesicles (arrows in Fig. 4C-x). We have ruled out PMN being these double-positive cells by examining their nuclear morphology but currently do not know their identity. TLR4 is also co-localized with AFP in AH (Fig. 4C-viii and xi) or albumin (Fig. 4C-ix and xii), suggesting the expression of TLR4 in liver progenitors and hepatocytes.

Spp1−/− mice develop AH

As *Spp1* implicated in AH (20, 21), was conspicuously upregulated in the HCFD+Alc +Binge AH livers, we tested the role of *Spp1* in the genesis of AH in the model. *Spp1*−/− and congenic WT male mice were subjected to the HCFD+Alc+Binge regimen in two repeated experiments each consisting 5–6 pairs of both genotypes. SPP1 deficiency did not affect hepatomegaly and BAL while it tended to increase splenomegaly ($p=0.10$) and to reduce plasma ALT ($p=0.13$) (Fig. 5A). Blind histological analysis revealed no differences in the incidence of PMN hepatitis (Fig. 5B), micro- and macro-vesicular steatosis, MNC inflammation (Table 2). However, we noted the most severe PMN infiltration (the grade 4 for each lobule containing PMN) in three of 10 *Spp1*−/− mice while none of 11 WT mice exhibited this severity (Table 2). Consistent with this observation, *Spp*−/− mice tended to have increased hepatic *Mpo* ($p=0.14$) and *Il-17a* ($p=0.09$) expression (Fig. 5C). *Il-22* was equally depleted and *Cxcl1* induced in both genotypes (Fig. 5C). We then counted the number of PMN infiltrated into the left, middle and right lobe sections of each mouse and expressed the PMN count per $100mm^2$. As shown in the right half of Fig. 5D, three *Spp1*−/− mice subjected to HCFD+Alc+Binge with the PMN grade of 4, had the higher counts of 200–215 PMN/$100mm^2$ while the rest had the counts similarly distributed in both genotyes, confirming SPP1 deficiency promoted the intensity of PMN infiltration in these three mice. Further, although *Mpo* and *Il-17a* upregulation in *Spp1*−/− mice did not achieve statistical significance due to the heterogeneous responses among the mice, *Mpo* and *Il-17a* inductions significantly and tightly correlated with the extent of PMN infiltration, and the three mice with the most severe AH had most accentuated increases in *Mpo* and *Il-17a* mRNA (red circles, Suppl. Fig. 2B). Fibrogenic genes (*Col1a1, Timp1*) and stemness genes (*Cd133, Nanog*) were equally induced in WT and *Spp1*−/− mice (Suppl. Fig. 2C).

We next tested the effect of SPP1 deficiency on chronic ASH produced by the HCFD+Alc regimen without binge. We noted no effects on BAL (252+37 in WT vs. 244+50 mg/dL in

Spp1−/−) and hepatomegaly (LW/BW: 0.1+0.006 in WT vs. 0.11+0.004 in *Spp1*−/−). Plasma ALT levels were significantly higher in *Spp1*−/− compared to WT mice (329+43 vs. 204+53 IU/L, $p<0.05$). More importantly, liver histology revealed that 3 out of 7 *Spp1*−/− mice developed intense PMN infiltration while none of 6 WT mice showed this change. The WT mice only had MNC infiltration (Fig. 5E). Careful PMN counting revealed that all WT mice with HCFD+Alc regimen had the liver PMN count of less than 28 per $100mm^2$, but the aforementioned three *Spp1*−/− mice had the PMN count of 76~120, the range seen in AH of WT mice subjected to HCFD+Alc+Binge (Fig. 5D). αSMA was similarly induced in WT and *Spp1*−/− mice subjected to HCFD+Alc or HCFD+Alc+Binge (Suppl. Fig. 2D). Collectively, these results suggest that SPP1 deficiency fails to prevent AH in the HCFD +Alc+Binge model but rather promotes the development of AH from chronic ASH in the HCFD+Alc model.

Discussions

To test the roles of SPP1 in ASH and AH, it was absolutely essential to establish clinically relevant animal models. The present study demonstrates that key pathological features seen in AH in patients are reproduced in mice by faithfully incorporating the risk factors associated with the disease. Habitual heavy alcohol was assured by *iG* ethanol infusion while Western diet consumption was implemented by *ad lib* intake of HCFD. These two factors induce chronic ASH primarily characterized by severe steatosis, MNC infiltration and fibrosis. This model was recently used to disclose a reversion of activated hepatic stellate cells to “inactivated” stellate cells with the vitamin A-replete status in resolution from alcoholic liver fibrosis (39). What was essential for the drastic shift of this pathology to AH, was repeated weekly alcohol binge which is a common behavior of patients with AH (1, 14, 15). Liver histology identified the features of AH including balloon cell degeneration and necrotic hepatocytes surrounded by PMN infiltrates. However, we did not observe the Mollory-Denk (M-D) bodies in the AH mouse livers, and this may be due to the fact that the mouse is resistant to the M-D body formation (40). Most notably, the model showed for the first time, clinical features of AH such as splenomegaly, hypoalbuminemia, and bilirubinemia. In mice with intensely inflamed livers as shown in Fig. 2C and Suppl. Fig. 1A, abdominal effusion was even noted. These changes are manifested in the background of chronic ASH typified by enhanced liver fibrosis (Fig. 2C and Suppl. Fig. 1B) as seen in AH patients.

Using *Spp1*−/− mice subjected to these models of chronic ASH and AH, we demonstrate global SPP1 deficiency triggers the genesis of AH in chronic ASH model (HCFD+Alc) and worsens the extent of PMN infiltration in some AH mice (HCFD+Alc+Binge). Based on these results, we have to conclude that SPP1 is protective rather than causal for AH. This conclusion is in contrast to the published study demonstrating that alcohol-fed *Spp1*−/− mice are protected from PMN infiltration (21). Among different possibilities for this discrepancy, the first and most obvious is that our models exhibit more severe and clinically relevant diseases while the model used previously produces milder and transient pathology (21). Our model is based on the synergism between the Western diet and alcohol with or without repeated binge. SPP1 may have differential actions based on the extent and nature of alcoholic liver pathology produced in these different models. Administration of anti-SPP1

antibody ameliorated liver injury caused by alcohol feeding and LPS injection in female rats (22). Although this two-hit model may produce acute liver inflammation similar to the binge-induced effect, our models tested the SPP1 deficiency during the genesis of chronic ASH or AH produced by the repeated binge insult in males but not in females. These differences may account for the discrepancy. Nonetheless, our findings based on the effects on both ASH and AH models, do not support the causal role of SPP1 in ASH or AH but rather reinforce the protective roles of SPP1 in ALD as proposed by others (26, 27).

In interpreting the SPP1 deficiency effects we observed, we must also consider alternative possibilities: SPP1 deficiency in other organs may have adverse outcome; or the *Spp1*−/− mice may have compensatory gene regulation which might have led to the pro-inflammatory outcome.

We noted despite the maximal control that the model provided over the feeding regimen, AH was not induced in all the mice and the degree of PMN infiltration was heterogeneous. Further, the promoting effects of SPP1 deficiency on PMN inflammation were seen in some but not all of the chronic ASH or AH mice. We do not know the reasons for these heterogeneous responses, but we consider these differential sensitivities must be what are observed in heavy drinkers. In this respect, our models should provide opportunities to search for the molecular basis for the predisposition for AH. Indeed, our results demonstrate the degree of *Il-17a* mRNA induction significantly and tightly correlates with AH in the HCFD+Alc+Binge WT and *Spp1*−/− mice, suggesting the role of LPS/TLR4-mediated IL-17a regulation in determining the predisposition.

What is equally intriguing is a striking depletion of IL-22 expression in our mouse AH. As IL-22 ameliorates alcoholic liver injury induced by chronic-binge ethanol feeding (18) and restricts liver fibrosis via induction of stellate cell senescence (36), IL-22 depletion may underlie accentuated hepatocellular death, inflammation and fibrosis in our mouse AH.

One cluster of genes upregulated in AH is that involved in stem cells and cancer. This is of particular interest not only because this unique change is associated with severe AH in patients (37) but also because these gene may be downstream of the TLR4 oncogenic pathway recently shown by us (17, 38). In this novel pathway, ectopic TLR4 activation induces stemness genes such as *Nanog, Oct4, and Sox2* to generate CD133+ tumor-initiating stem cell-like cells (TICs) and liver tumors (17, 38). In the AH model, TLR4 expression and activation are heightened and are associated with upregulation of *Cd133* and *Nanog*. Further, TLR4 overexpression is co-localized with albumin and AFP, suggesting that hepatocytes or hepatoblasts are targeted by this pathway as previously shown in alcohol-fed HCV *NS5A* transgenic mice (17). A recent study suggests a notion that dysplastic hepatocytes due to hepatotoxicity may generate progenitor-type cells via compensatory proliferation in pre-neoplastic lesions (41). The observed TLR4+AFP+ and TLR4+NANOG + cells in the mouse AH livers (Fig. 4C) may represent such progenitor cells or TICs which are generated from dysplastic hepatocytes with activated TLR4. Moreover, studies on the interactions between proinflammatory and pro-oncogenic actions of IL-17a (42) with the TLR4 pathway, may help disclose novel mechanisms for the link between inflammation and carcinogenesis in ALD.

Supplementary Material

Refer to Web version on PubMed Central for supplementary material.

Acknowledgements

We would like to thank Akiko Ueno and Rylee Do for their technical support.

Supported by P50AA011999 (Animal and Morphology Core, HT), U01AA018663 (HT), 1I01BX001991 (HT), AA0188857 (KM), K01AA020524 (JX), and U01AA21898 (SF), Medical Research Service of Department of Veterans Affairs, the Histology and Microscopy Core of the USC Research Center for Liver Diseases (P30DK048522), and a grant from Suntory Global Innovation Center Ltd.

Abbreviations

ALD	alcoholic liver disease
AH	alcoholic hepatitis
ASH	alcoholic steatohepatitis
PMN	polymorphonuclear
MYO	myeloperoxidase
SPP1	osteopontin
HCV	hepatitis C virus
HBV	hepatitis B virus
TLR4	toll-like receptor-4
AST	aspartate aminotransferase
ALT	alanine aminotransferase
IL	interleukin
Cxcl1	chemokine (C-X-C motif) ligand 1
CD133	cluster of differentiation-133
Epcam	epithelial cell adhesion molecule
LPS	lipopolysaccharide
RNA	ribonucleic acid
cDNA	complementary deoxyribonucleic acid
qPCR	quantitative polymerase chain reaction
TAK1	TGF-beta activated kinase 1
TRAF6	TNF receptor-associated factor 6
Timp1	tissue inhibitor for metalloproteinase 1
AFP	alpha-fetal protein.

References

1. Choi G, Runyon BA. Alcoholic hepatitis: a clinician's guide. Clin Liver Dis. 2012 May; 16(2):371–385. [PubMed: 22541704]
2. Maddrey WC, Boitnott JK, Bedine MS, Weber FL Jr, Mezey E, White RI Jr. Corticosteroid therapy of alcoholic hepatitis. Gastroenterology. 1978 Aug; 75(2):193–199. [PubMed: 352788]
3. O'Shea RS, Dasarathy S, McCullough AJ. Alcoholic liver disease. Hepatology. 2010 Jan; 51(1): 307–328. [PubMed: 20034030]
4. Liangpunsakul S. Clinical characteristics and mortality of hospitalized alcoholic hepatitis patients in the United States. J Clin Gastroenterol. 2011 Sep; 45(8):714–719. [PubMed: 21085006]
5. Mathurin P, Lucey MR. Management of alcoholic hepatitis. J Hepatol. 2012; 56(Suppl 1):S39–S45. [PubMed: 22300464]
6. Singal AK, Kamath PS, Gores GJ, Shah VH. Alcoholic Hepatitis: Current Challenges and Future Directions. Clin Gastroenterol Hepatol. 2013 Jun 28.
7. Gao B, Bataller R. Alcoholic liver disease: pathogenesis and new therapeutic targets. Gastroenterology. 2011 Nov; 141(5):1572–1585. [PubMed: 21920463]
8. Raynard B, Balian A, Fallik D, Capron F, Bedossa P, Chaput JC, et al. Risk factors of fibrosis in alcohol-induced liver disease. Hepatology. 2002 Mar; 35(3):635–638. [PubMed: 11870378]
9. Naveau S, Giraud V, Borotto E, Aubert A, Capron F, Chaput JC. Excess weight risk factor for alcoholic liver disease. Hepatology. 1997 Jan; 25(1):108–111. [PubMed: 8985274]
10. Xu J, Lai KK, Verlinsky A, Lugea A, French SW, Cooper MP, et al. Synergistic steatohepatitis by moderate obesity and alcohol in mice despite increased adiponectin and p-AMPK. J Hepatol. 2011 Sep; 55(3):673–682. [PubMed: 21256905]
11. Singal AK, Anand BS. Mechanisms of synergy between alcohol and hepatitis C virus. J Clin Gastroenterol. 2007 Sep; 41(8):761–772. [PubMed: 17700425]
12. Poynard T, Bedossa P, Opolon P. Natural history of liver fibrosis progression in patients with chronic hepatitis C. The OBSVIRC, METAVIR, CLINIVIR, and DOSVIRC groups. Lancet. 1997 Mar 22; 349(9055):825–832. [PubMed: 9121257]
13. Singal AK, Sagi S, Kuo YF, Weinman S. Impact of hepatitis C virus infection on the course and outcome of patients with acute alcoholic hepatitis. Eur J Gastroenterol Hepatol. 2011 Mar; 23(3): 204–209. [PubMed: 21258239]
14. Ceccanti M, Attili A, Balducci G, Attilia F, Giacomelli S, Rotondo C, et al. Acute alcoholic hepatitis. J Clin Gastroenterol. 2006 Oct; 40(9):833–841. [PubMed: 17016141]
15. Zakhari S, Li TK. Determinants of alcohol use and abuse: Impact of quantity and frequency patterns on liver disease. Hepatology. 2007 Dec; 46(6):2032–2039. [PubMed: 18046720]
16. Ueno A, Lazaro R, Wang PY, Higashiyama R, Machida K, Tsukamoto H. Mouse intragastric infusion (iG) model. Nat Protoc. 2012 Apr; 7(4):771–781. [PubMed: 22461066]
17. Machida K, Tsukamoto H, Mkrtchyan H, Duan L, Dynnyk A, Liu HM, et al. Toll-like receptor 4 mediates synergism between alcohol and HCV in hepatic oncogenesis involving stem cell marker Nanog. Proc Natl Acad Sci U S A. 2009 Feb 3; 106(5):1548–1553. [PubMed: 19171902]
18. Ki SH, Park O, Zheng M, Morales-Ibanez O, Kolls JK, Bataller R, et al. Interleukin-22 treatment ameliorates alcoholic liver injury in a murine model of chronic-binge ethanol feeding: role of signal transducer and activator of transcription 3. Hepatology. 2010 Oct; 52(4):1291–1300. [PubMed: 20842630]
19. Bertola A, Park O, Gao B. Chronic plus binge ethanol feeding synergistically induces neutrophil infiltration and liver injury in mice: A critical role for E-selectin. Hepatology. 2013 Mar 26.
20. Apte UM, Banerjee A, McRee R, Wellberg E, Ramaiah SK. Role of osteopontin in hepatic neutrophil infiltration during alcoholic steatohepatitis. Toxicol Appl Pharmacol. 2005 Aug 22; 207(1):25–38. [PubMed: 15885730]
21. Morales-Ibanez O, Dominguez M, Ki SH, Marcos M, Chaves JF, Nguyen-Khac E, et al. Human and experimental evidence supporting a role for osteopontin in alcoholic hepatitis. Hepatology. 2013 May 31.

22. Banerjee A, Apte UM, Smith R, Ramaiah SK. Higher neutrophil infiltration mediated by osteopontin is a likely contributing factor to the increased susceptibility of females to alcoholic liver disease. J Pathol. 2006 Mar; 208(4):473–485. [PubMed: 16440289]
23. Patouraux S, Bonnafous S, Voican CS, Anty R, Saint-Paul MC, Rosenthal-Allieri MA, et al. The osteopontin level in liver, adipose tissue and serum is correlated with fibrosis in patients with alcoholic liver disease. PLoS One. 2012; 7(4):e35612. [PubMed: 22530059]
24. Koh A, da Silva AP, Bansal AK, Bansal M, Sun C, Lee H, et al. Role of osteopontin in neutrophil function. Immunology. 2007 Dec; 122(4):466–475. [PubMed: 17680800]
25. Syn WK, Choi SS, Liaskou E, Karaca GF, Agboola KM, Oo YH, et al. Osteopontin is induced by hedgehog pathway activation and promotes fibrosis progression in nonalcoholic steatohepatitis. Hepatology. 2011 Jan; 53(1):106–115. [PubMed: 20967826]
26. Ge X, Leung TM, Arriazu E, Lu Y, Urtasun R, Christensen B, et al. Osteopontin binding to lipopolysaccharide lowers tumor necrosis factor-alpha and prevents early alcohol-induced liver injury in mice. Hepatology. 2014 Apr; 59(4):1600–1616. [PubMed: 24214181]
27. Ge X, Lu Y, Leung TM, Sorensen ES, Nieto N. Milk osteopontin, a nutritional approach to prevent alcohol-induced liver injury. Am J Physiol Gastrointest Liver Physiol. 2013 May 15; 304(10):G929–G939. [PubMed: 23518682]
28. Maltby J, Wright S, Bird G, Sheron N. Chemokine levels in human liver homogenates: associations between GRO alpha and histopathological evidence of alcoholic hepatitis. Hepatology. 1996 Nov; 24(5):1156–1160. [PubMed: 8903391]
29. Dominguez M, Miquel R, Colmenero J, Moreno M, Garcia-Pagan JC, Bosch J, et al. Hepatic expression of CXC chemokines predicts portal hypertension and survival in patients with alcoholic hepatitis. Gastroenterology. 2009 May; 136(5):1639–1650. [PubMed: 19208360]
30. Lafdil F, Miller AM, Ki SH, Gao B. Th17 cells and their associated cytokines in liver diseases. Cell Mol Immunol. 2010 Jul; 7(4):250–254. [PubMed: 20305686]
31. Lemmers A, Moreno C, Gustot T, Marechal R, Degre D, Demetter P, et al. The interleukin-17 pathway is involved in human alcoholic liver disease. Hepatology. 2009 Feb; 49(2):646–657. [PubMed: 19177575]
32. Meng F, Wang K, Aoyama T, Grivennikov SI, Paik Y, Scholten D, et al. Interleukin-17 signaling in inflammatory, Kupffer cells, and hepatic stellate cells exacerbates liver fibrosis in mice. Gastroenterology. 2012 Sep; 143(3):765–776. [PubMed: 22687286]
33. Scheiermann P, Bachmann M, Goren I, Zwissler B, Pfeilschifter J, Muhl H. Application of interleukin-22 mediates protection in experimental acetaminophen-induced acute liver injury. Am J Pathol. 2013 Apr; 182(4):1107–1113. [PubMed: 23375450]
34. Zindl CL, Lai JF, Lee YK, Maynard CL, Harbour SN, Ouyang W, et al. IL-22-producing neutrophils contribute to antimicrobial defense and restitution of colonic epithelial integrity during colitis. Proc Natl Acad Sci U S A. 2013 Jul 30; 110(31):12768–12773. [PubMed: 23781104]
35. Feng D, Kong X, Weng H, Park O, Wang H, Dooley S, et al. Interleukin-22 promotes proliferation of liver stem/progenitor cells in mice and patients with chronic hepatitis B virus infection. Gastroenterology. 2012 Jul; 143(1):188–198. [PubMed: 22484119]
36. Kong X, Feng D, Wang H, Hong F, Bertola A, Wang FS, et al. Interleukin-22 induces hepatic stellate cell senescence and restricts liver fibrosis in mice. Hepatology. 2012 Sep; 56(3):1150–1159. [PubMed: 22473749]
37. Sancho-Bru P, Altamirano J, Rodrigo-Torres D, Coll M, Millan C, Jose LJ, et al. Liver progenitor cell markers correlate with liver damage and predict short-term mortality in patients with alcoholic hepatitis. Hepatology. 2012 Jun; 55(6):1931–1941. [PubMed: 22278680]
38. Chen CL, Tsukamoto H, Liu JC, Kashiwabara C, Feldman D, Sher L, et al. Reciprocal regulation by TLR4 and TGF-beta in tumor-initiating stem-like cells. J Clin Invest. 2013 Jul 1; 123(7):2832–2849. [PubMed: 23921128]
39. Kisseleva T, Cong M, Paik Y, Scholten D, Jiang C, Benner C, et al. Myofibroblasts revert to an inactive phenotype during regression of liver fibrosis. Proc Natl Acad Sci U S A. 2012 Jun 12; 109(24):9448–9453. [PubMed: 22566629]
40. Yuan QX, Marceau N, French BA, Fu P, French SW. Mallory body induction in drug-primed mouse liver. Hepatology. 1996 Sep; 24(3):603–612. [PubMed: 8781332]

41. He G, Dhar D, Nakagawa H, Font-Burgada J, Ogata H, Jiang Y, et al. Identification of liver cancer progenitors whose malignant progression depends on autocrine IL-6 signaling. Cell. 2013 Oct 10; 155(2):384–396. [PubMed: 24120137]

42. Gu FM, Li QL, Gao Q, Jiang JH, Zhu K, Huang XY, et al. IL-17 induces AKT-dependent IL-6/JAK2/STAT3 activation and tumor progression in hepatocellular carcinoma. Mol Cancer. 2011; 10:150. [PubMed: 22171994]

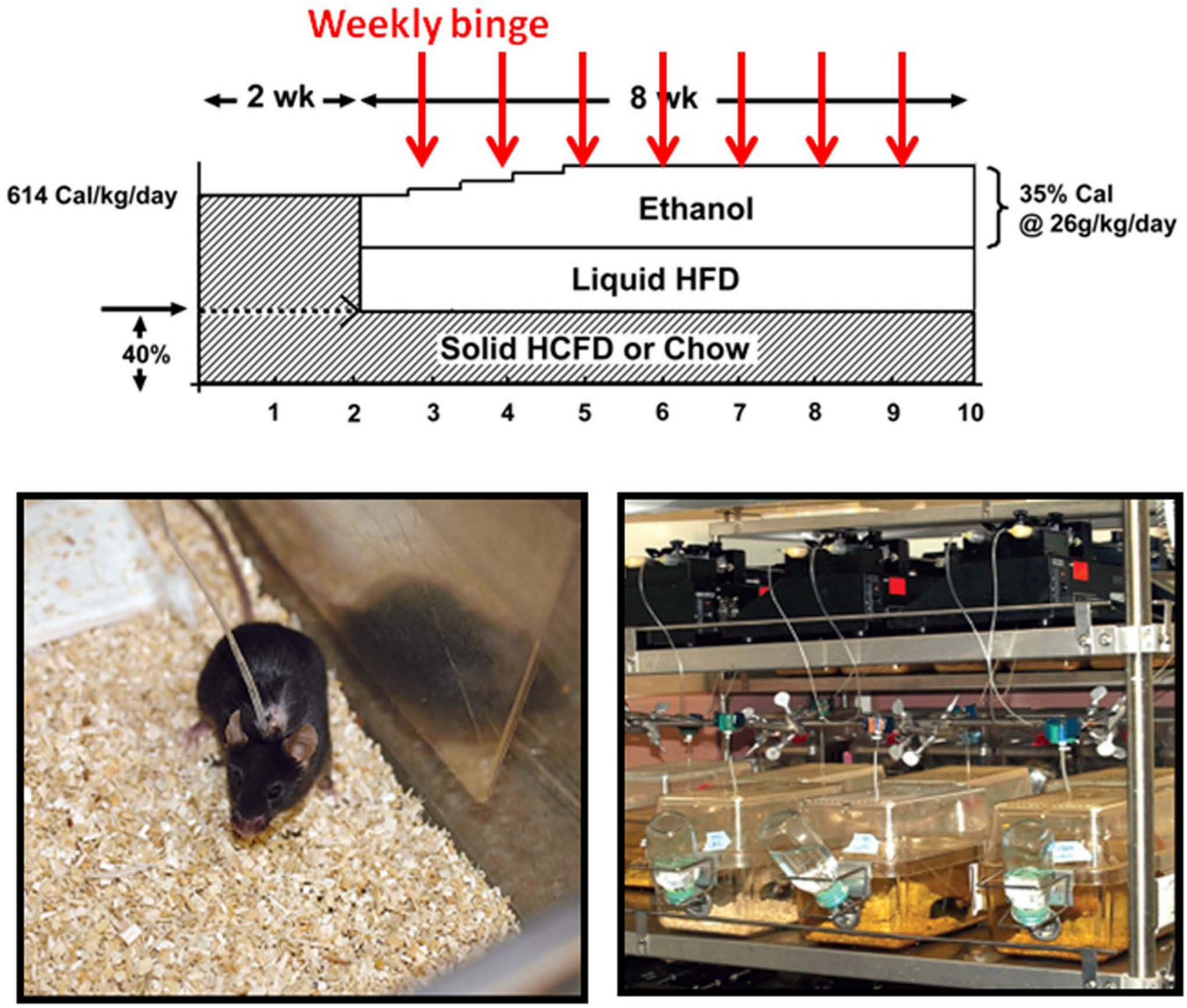

Fig. 1.

The upper diagram depicts the *ad lib* and *iG* "hybrid" feeding regimen of HCFD and ethanol liquid diet with or without weekly binge administration of alcohol. The lower two photos show an individual *iG* mouse under this regimen (left) and an infusion set-up (right).

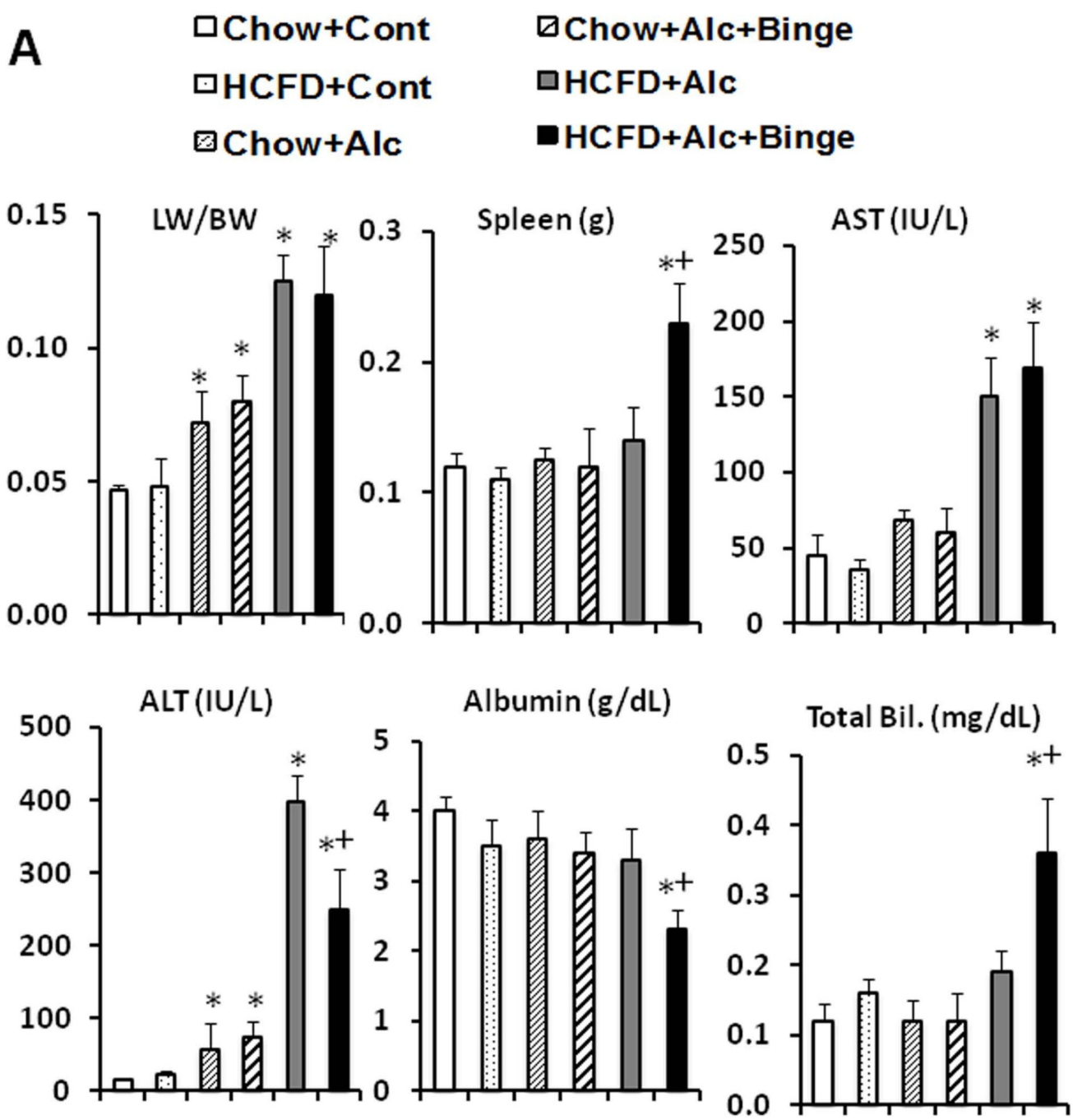

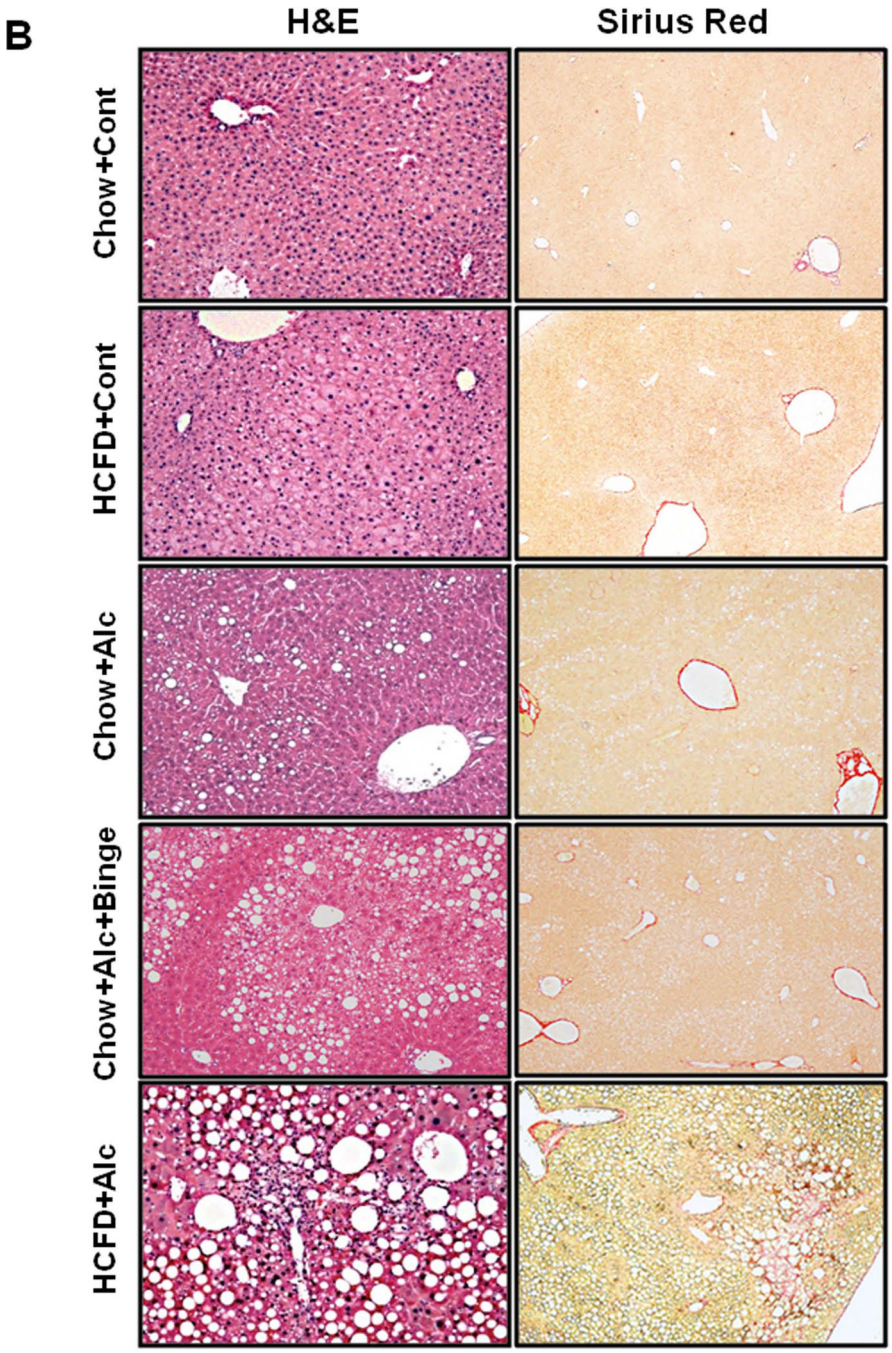

C

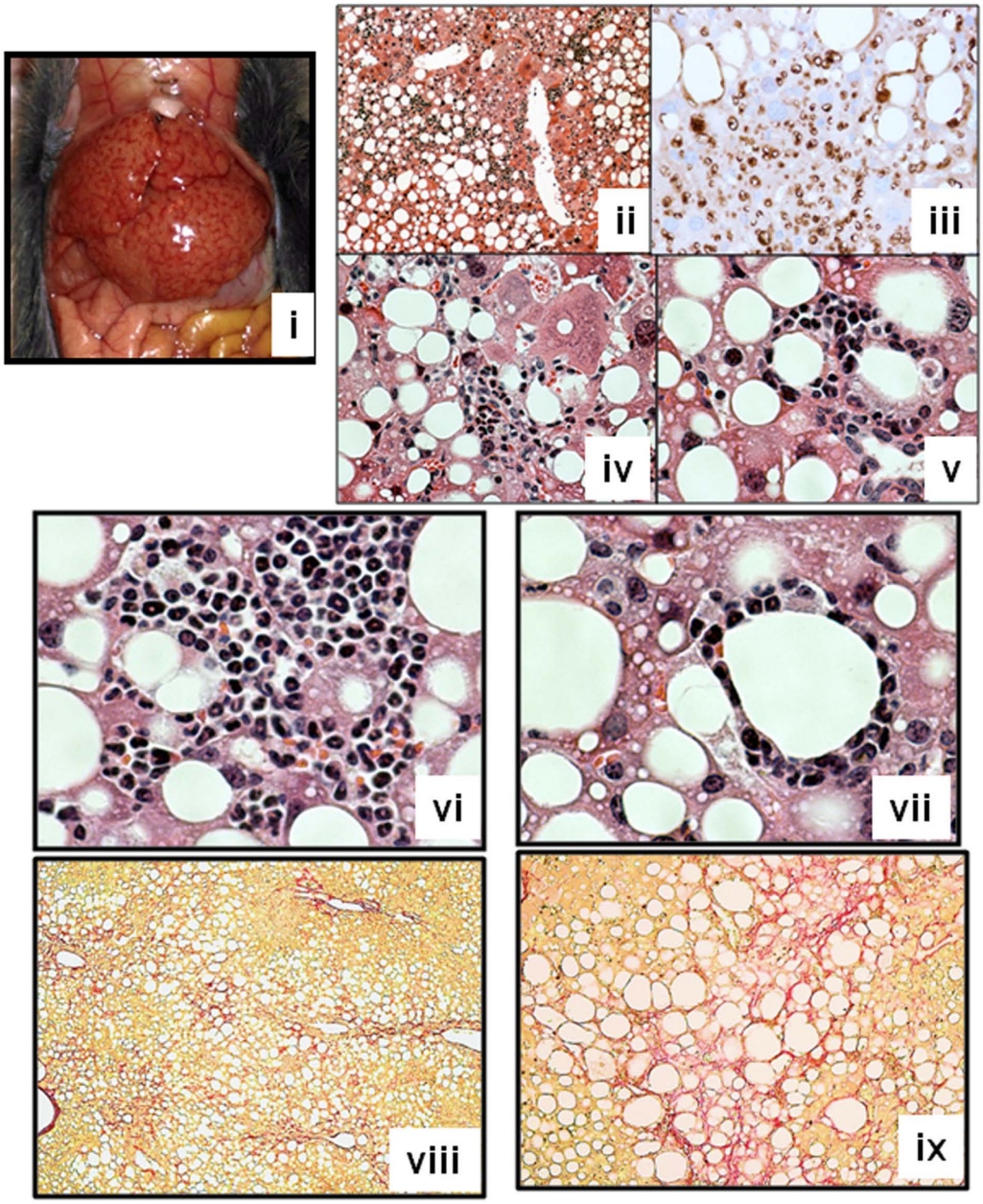

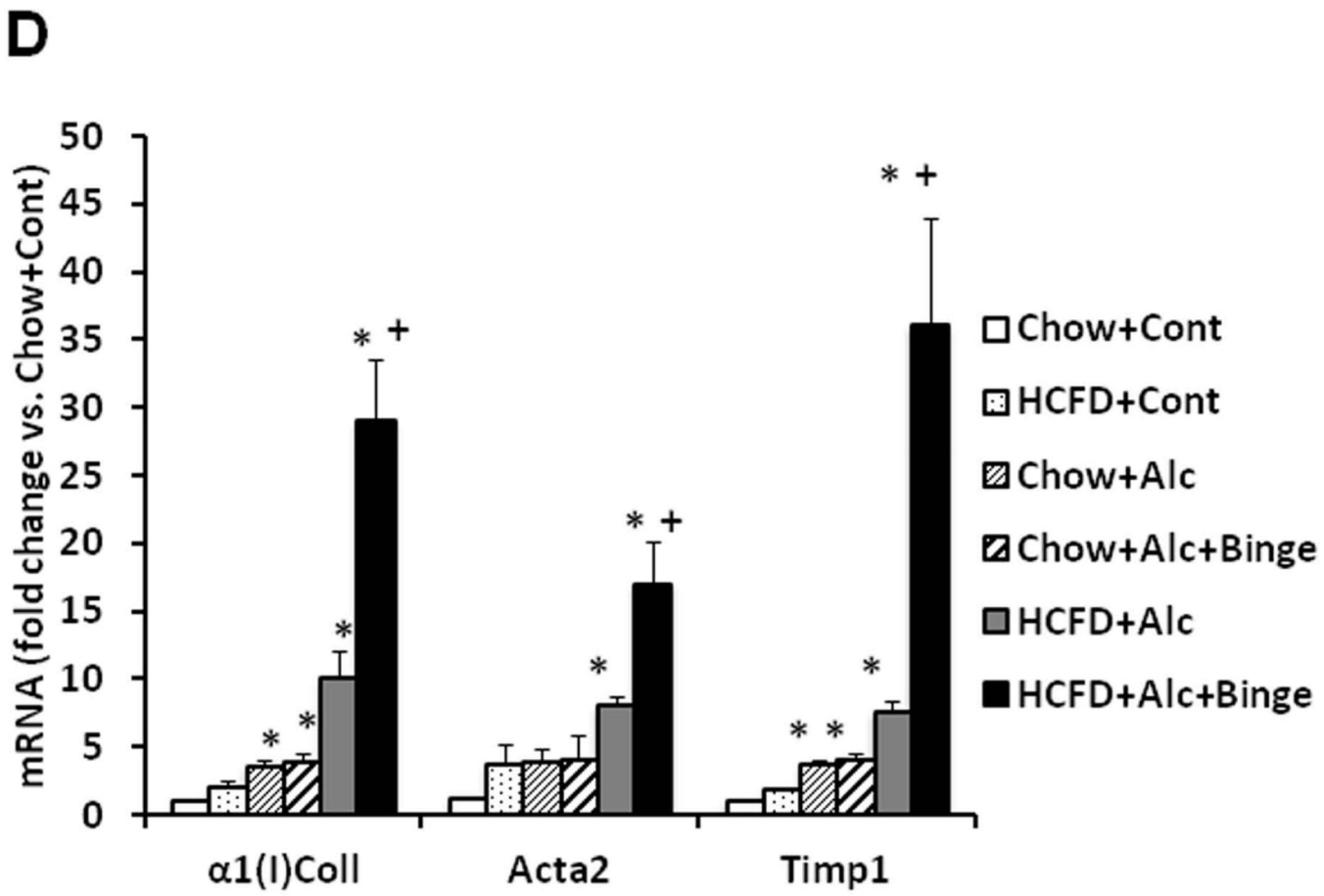

Fig. 2.

A. Synergistic increases in the liver weight/body weight and plasma ALT and AST levels are noted in HCFD+Alc and HCFD+Alc+Binge mice. Splenomegaly, hypoalbuminemia, and hyperbilirubinemia are noted only in HCFD+Alc+Binge mice. *p<0.05 compared to Chow+Cont; +p<0.05 compared to HCFD+Alc. **B.** Representative lower power images of the liver stained with H&E and Sirius red. ASH with mononuclear cell inflammation and liver fibrosis is noted in the HCFD+Alc mouse. x100 magnification. **C.** A representative gross photo of the markedly enlarged and inflamed HCFD+Alc+Binge mouse liver (i). Diffuse and intense PMN parenchymal infiltration in the HCFD+Alc+Binge mice, ×100 (ii). Chloracetate esterase (CEA) staining confirms PMNs infiltrating into the liver parenchyma, ×200 (iii). PMN infiltration often surrounds necrotic or degenerating foamy hepatocytes, ×200 and ×400 (iv and v). Massive PMN infiltration with necrotic hepatoyctes, ×400 (vi). PMN encircling a degenerative hepatocyte forming “satellitosis”, ×600 (vii). Sirius red staining demonstrates pericellular and perisinusoidal liver fibrosis, ×100 and ×200 (viii and ix). **D.** Fibrogenic genes, *1(I)Coll*, *Sma (Acta2)*, and *Timp1* are induced in HCFD+Alc and further upregulated in HCFD+Alc+Binge livers. *p<0.05 compared to Chow+Cont; +p<0.05 compared to HCFD+Alc.

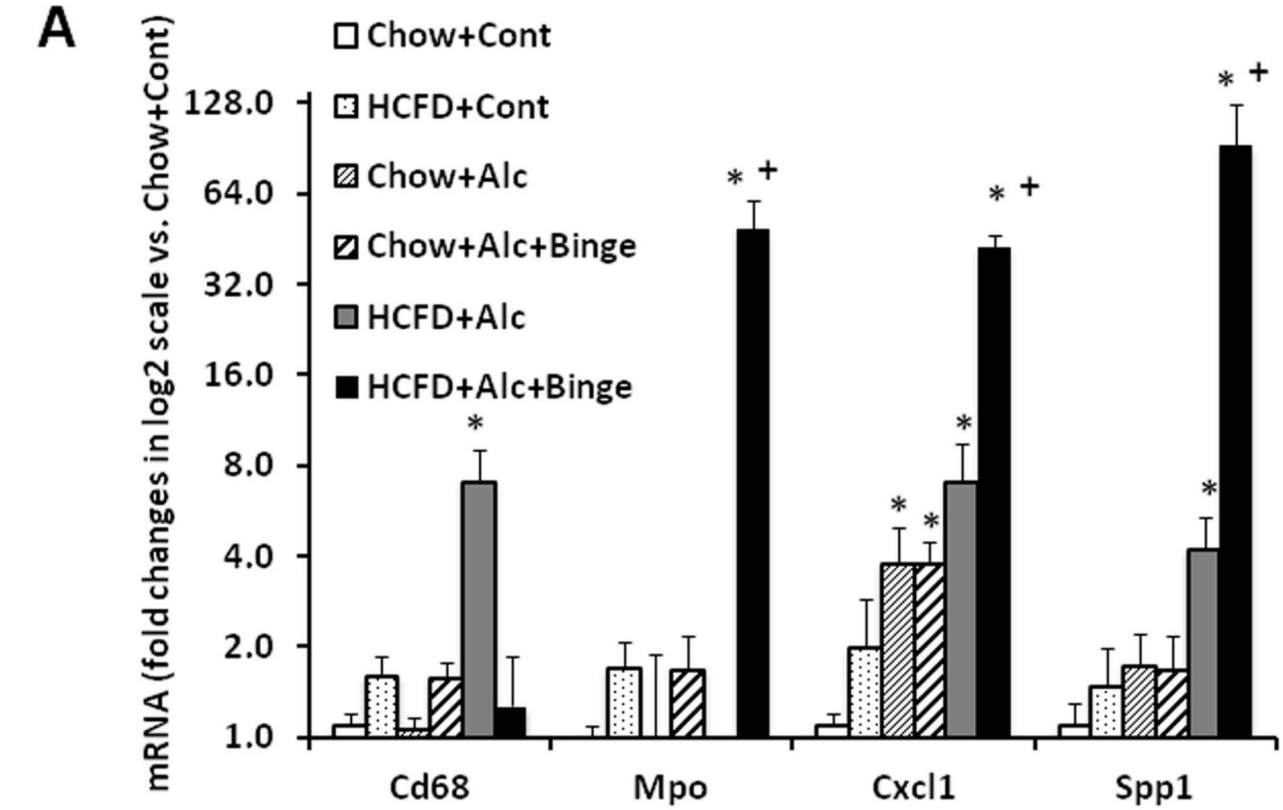

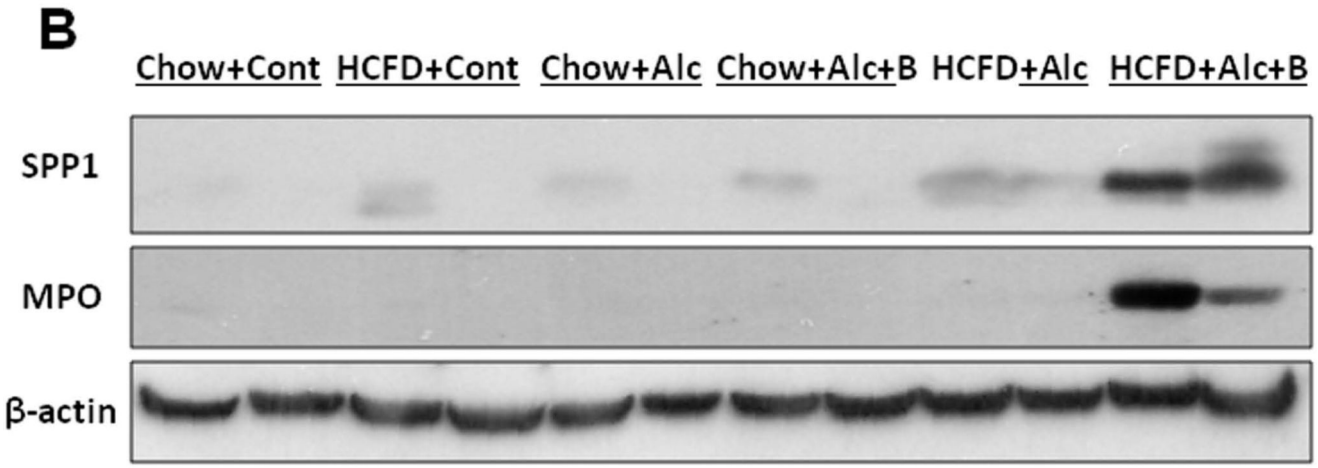

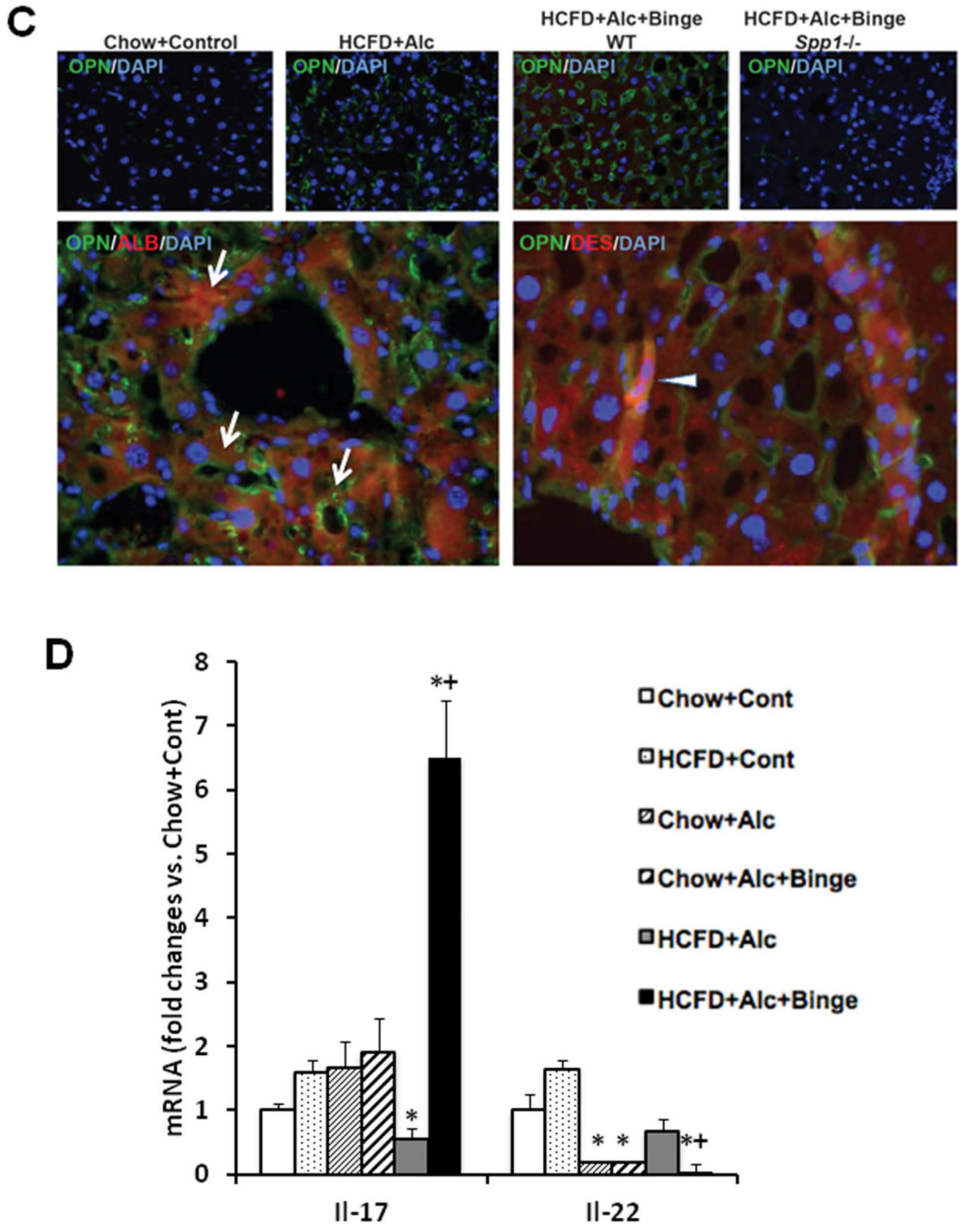

Fig. 3.

A. Liver qPCR analysis validates PMN infiltration in HCFD+Alc+Binge mice by conspicuous inductions of myeloperoxidase (*Mpo*) and PMN chemokines such as Gro-α (*Cxcl1*) and osteopontin (*Spp1*). Cd68, the marker for activated macrophages, is upregulated only in HCFD+Alc. *p<0.05 compared to Chow+Cont; +p<0.05 compared to HCFD+Alc +Binge. **B.** Immunoblotting analysis confirms marked SPP1 and MPO inductions in HCFD +Alc+Binge. **C.** Immunofluorescent microscopy demonstrates increased staining for SPP1 (OPN) in HCFD+Alc as compared to Chow+Cont (two left upper images, ×40). SPP1

(OPN) induction is further enhanced in WT mouse but not in *Spp1*−/− mouse subjected to HCFD+Alc+Binge (two right upper images, ×40). A high-power view of dual staining for SPP1 (OPN) and Albumin (ALB) reveals the expression of SPP1 in centrilobular hepatocytes containing intracellular fat vesicles (arrows, left lower image, ×400). SPP1 and desmin (DES) dual staining revels hepatic stellate cells expressing SPP1 (arrowhead, right lower image, ×600). **D.** Hepatic mRNA expression of IL-17a is markedly increased while that of IL-22 reduced in HCFD+Alc+Binge mice. *p<0.05 compared to Chow+Cont; +p<0.05 compared to HCFD+Alc.

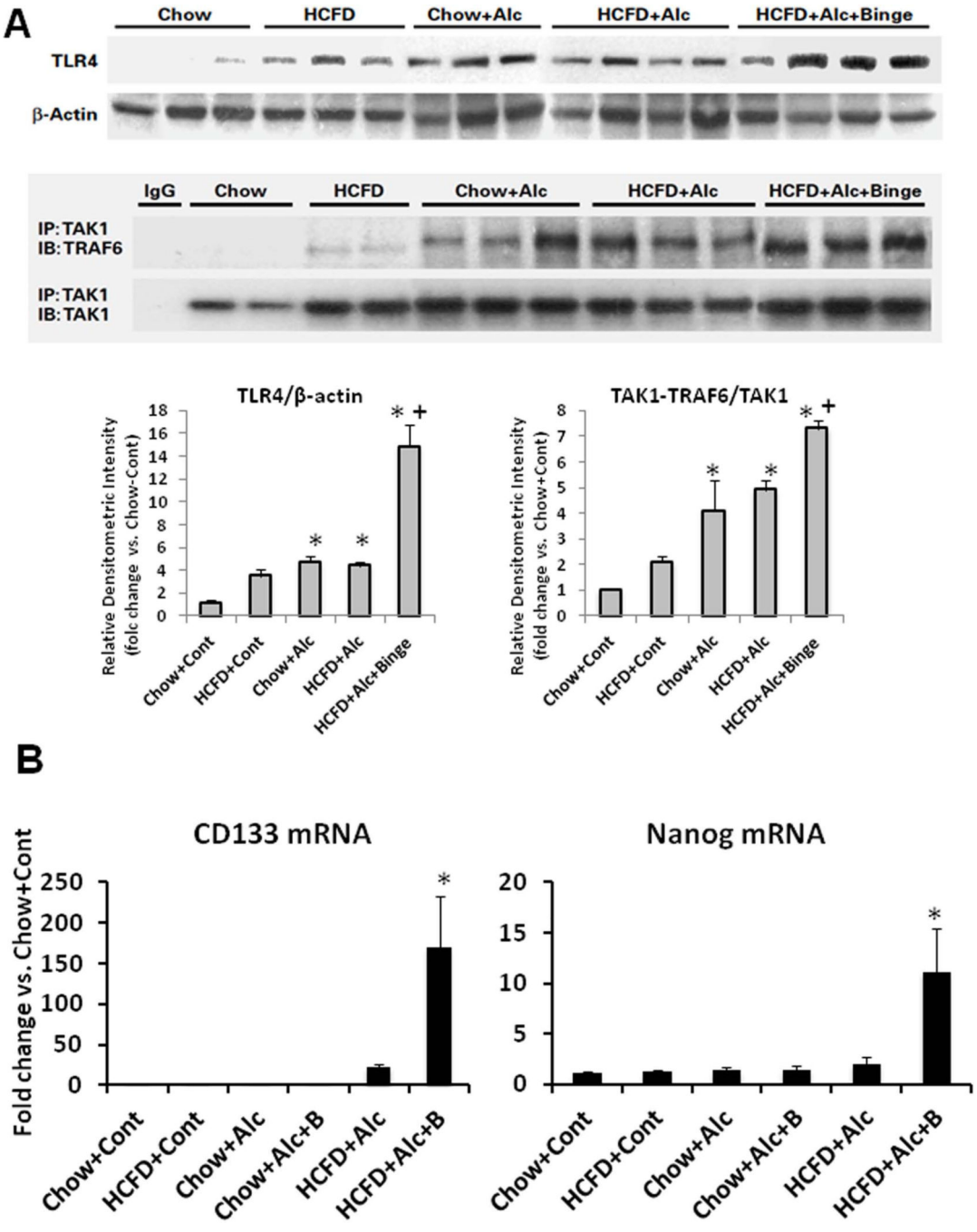

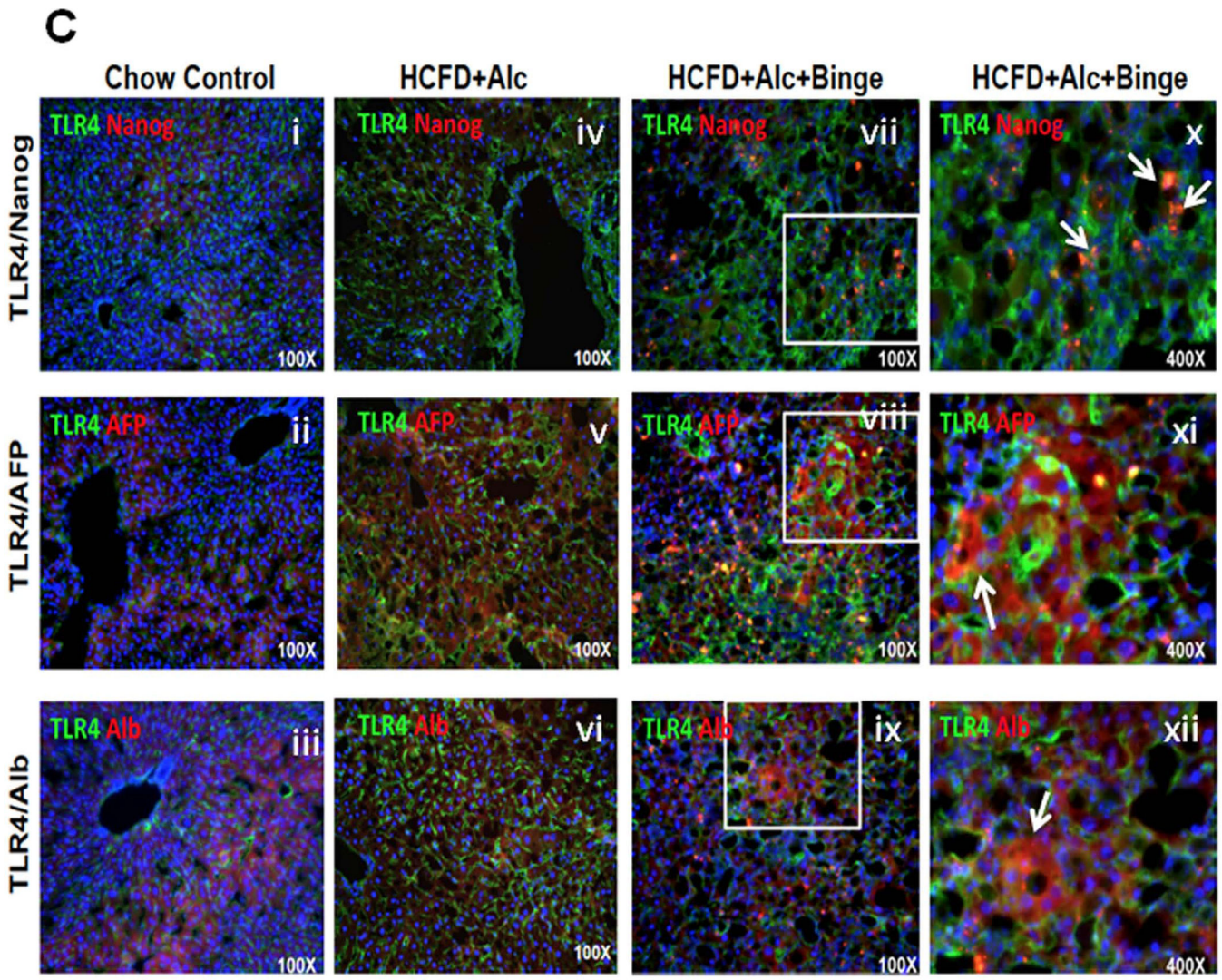

Fig. 4.

A. TLR4 expression and its activation assessed by immunobotting and co-IP of TRAF6 and TAK1 are most conspicuous in HCFD+Alc+Binge mouse livers. Bar graphs below show densitometric data obtained by normalization to β-actin or TAK1 and comparison to Chow +Cont. *p<0.05 compared to Chow+Cont; +p<0.05 compared to HCFD+Alc. **B.** Stemness genes downstream of TLR4 such as *Cd133* and *Nanog*, are markedly induced in HCFD+Alc +Binge livers. *p<0.05 compared to other groups. **C.** Immunofluorescent microscopy reveals increased sinusoidal TLR expression but no NANOG expression in HCFD+Alc (iv vs. i). TLR4 staining is intensified and appearance of NANOG positivity in HCFD+Alc +Binge (vii). Higher magnification of a white square area (x) reveals small cells with NANOG positivity around hepatocytes with large fat vesicles (arrows). TLR4 expression is seen in AFP-positive cells (viii and arrow in xi) and albumin-positive cells (ix and arrow in xii) in HCFD+Alc+Binge. ×40 magnification for i–ix and ×400 for x–xii.

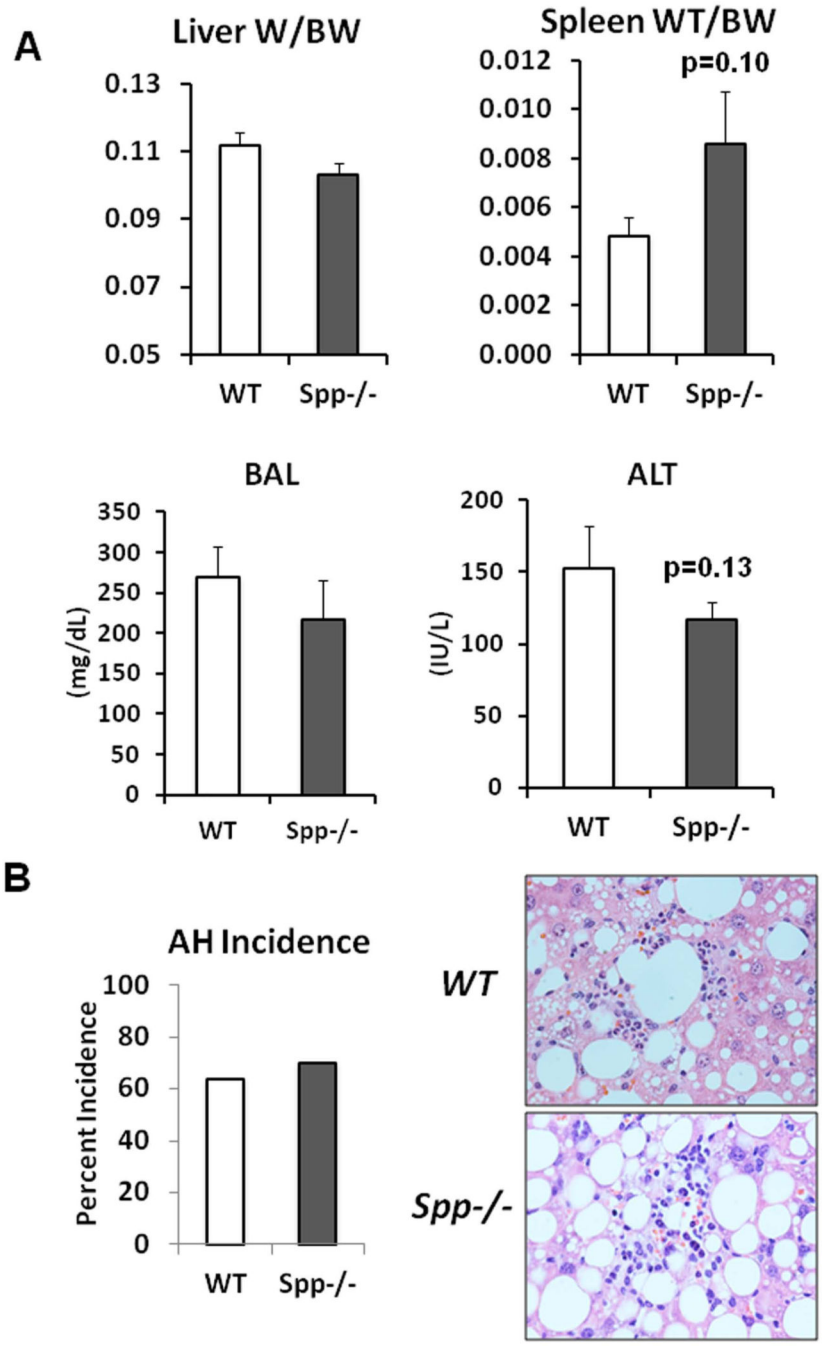

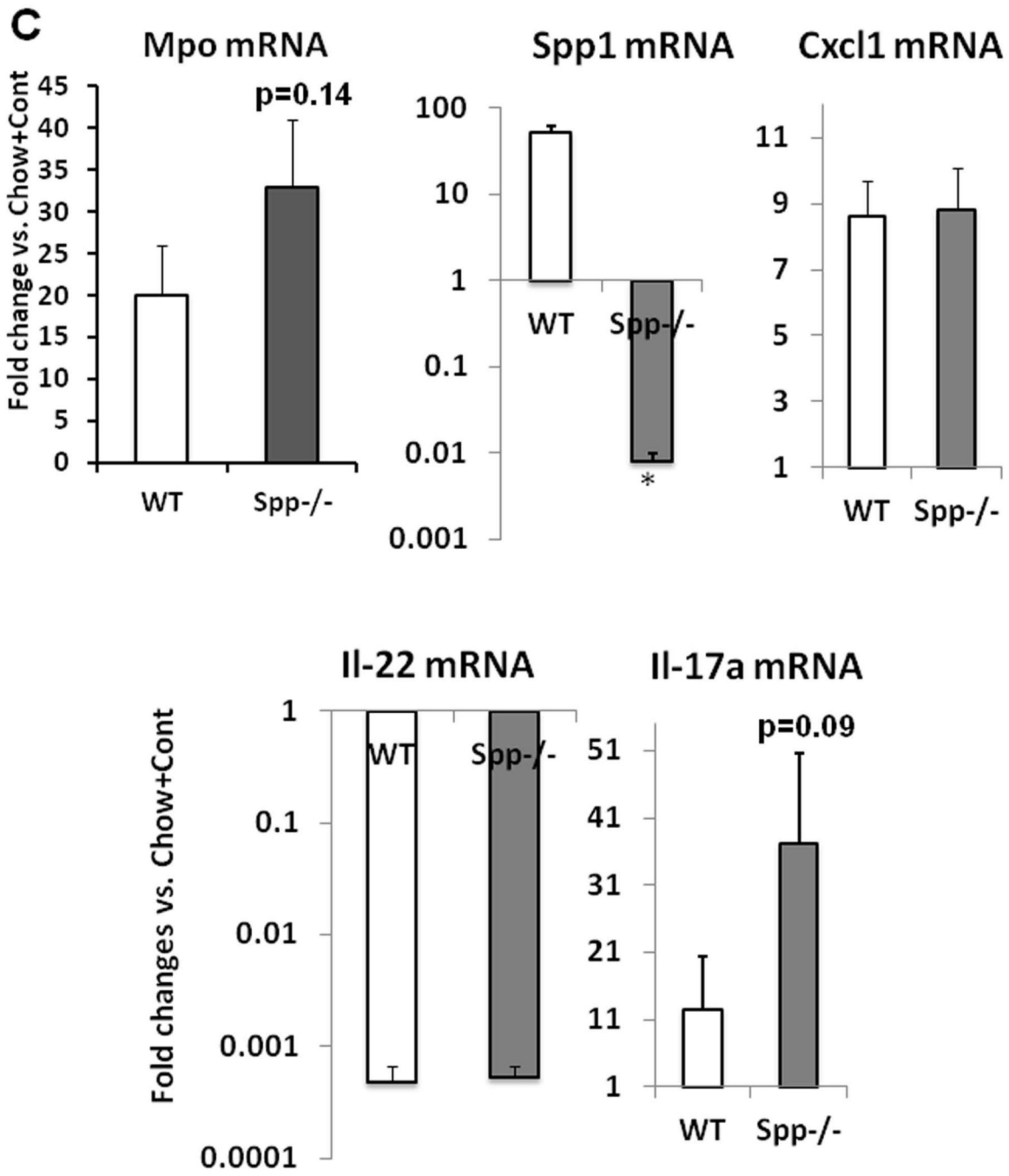

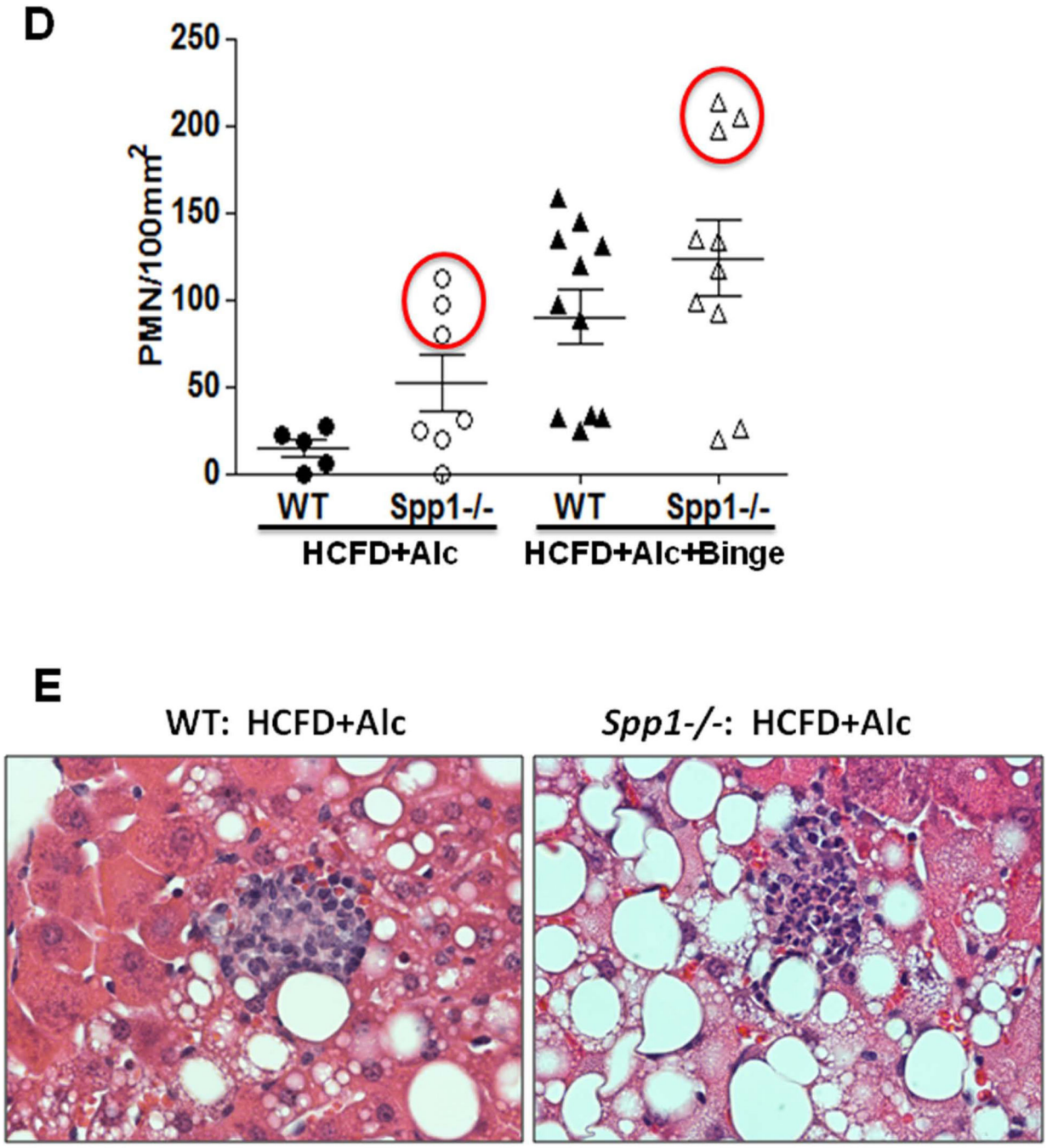

Fig. 5.

A. Osteopontin deficiency (*Spp*−/−) does not affect hepatomegaly and blood alcohol concentrations (BAL) by the HCFD+Alc+Binge regimen as compared to WT mice. Splenomegaly tends to be worsened and plasma ALT tends to be reduced in *Spp*−/− compared to WT. **B.** The incidence of AH is not altered in *Spp*−/− mice (left). Representative H&E stained images of AH for both genotypes are shown in right (×200). **C.** Hepatic mRNA levels of *Myo* and *Il-17a* tend to be higher in *Spp*−/− mice subjected to HCFD+Alc+Binge compared to WT mice while *Cxcl1* is similarly induced and *Il-22*

repressed in both genotypes. All data expressed as fold changes compared to Chow+Cont, *p<0.05. **D**. Scatter plots for PMN count per 100mm^2 derived by examining sections from the three major liver lobes (left, middle, right), reveal low background PMN counts in WT mice subjected to HCFD+Alc and increased counts in WT mice subjected to HCFD+Alc +Binge, confirming the incidence of AH in the latter. Note three *Spp1*−/− mice subjected to HCFD+Alc have high PMN counts within the range observed in WT HCFD+Alc+Binge mice (left red circle). Also note that three of *Spp1*−/− HCFD+Alc+Binge mice have higher PMN counts compared to WT mice (right red circle). **E.** Representative microphotographs of AH induced in a *Spp1*−/− mouse subjected to the HCFD+Alc regimen (right) as opposed to chronic ASH with MNC infiltration in a WT mouse (left), H&E staining, ×400.

Table 1

A. Differentially regulated genes by functions in AH vs. ASH livers.

Category	p-value	# genes
Upregulated genes		
Stem cells and Cancer	4.63E-22 – 1.73E-03 1	89
Inflammation	4.35E-17 – 1.69E-03	102
Connective Diseases	6.32E-15 – 1.69E-03	75
Downregulated genes		
Drug Metabolism	4.33E-04– 3.52E-02	34
Lipid Metabolism	4.22E-09 - 3.52E-02	64
Transport	5.00E-06 - 3.52E-02	55

B. PMN-related genes (in bold) among top 10 upregulated genes in AH vs. ASH.

Gene	Fold Increase
Neutrophilic granule protein	**31.9**
Myeloperoxidase	**14.9**
Lactoferrin	**13.8**
H19 fetal liver mRNA	13.4
RIKEN cDNA 1830127L07	12.8
Cathepsin G	**11.4**
Calgranulin A	**10.8**
Elastase (neutrophilic)	**10.4**
MMP7	**9.6**
Calgranulin B	**8.1**

Table 2

Blind liver histological grading of WT and Spp1−/−1 mice subjected to HCFD+Alc+Binge: Macro, microvesicular; Micro, microvesicular; MNC, mononuclear cells.

	Liver Histology			
	Steatosis		Inflammation	
WT	**Macro**	**Micro**	**MNC**	**PMN**
3866	4	1	3	1
3868	4	1	3	1
3870	3	3	4	1
3871	4	1	4	2
3875	4	1	1	0
3876	4	2	3	0
3877	4	1	2	0
3878	4	1	2	0
4007	4	1	3	2
4009	4	1	2	1
4010	3	0.5	2	3
Spp1−/−				
3861	4	1	1	0
3862	3	2	4	4
3863	4	2	1	0
3872	4	1	4	4
3874	4	1	2	0
3879	3	1	3	2
4002	4	1	1	1
4003	3	1	1	1
4004	4	0.5	2	1
4005	4	1	2	4